doi:10.2533/chimia.2024.845 Chimia 78 (2024) 845–854

Electrified Enhanced Recovery of Lithium from Unconventional Sources

Harris E. Kohl[a], Carlos A. Larriuz[a], Andrew Ezazi[a], Mohammed Al-Hashimi[b], Hassan S. Bazzi[b], and Sarbajit Banerjee[b–d*]

Abstract: Demand for lithium is expected to quadruple by the end of the decade. Without new sources of production, the supply-demand curve is expected to invert. Traditional geological reserves will not be able to meet the anticipated gap, thus unconventional sources of lithium will need to be utilized, setting the stage for fierce competition for perhaps the most critical of mineral resources required for the energy transition. Direct Lithium Extraction refers to the umbrella of technologies being developed to access lithium from unconventional sources. Electrochemical extraction offers significant promise for its selectivity and low operating cost when coupled with renewable energy. This review aims to describe materials and process design considerations for electrochemical extraction of lithium from aqueous sources with a specific emphasis on ζ-V_2O_5 designed in our research group as an insertion host. We point to specific strategies for improving capacity and selectivity for electrochemical lithium extraction based on materials design across length scales. Strategies range from site-selective modification of insertion hosts to controlled tortuosity of ion diffusion pathways in porous electrode architectures. Electrochemical lithium extraction from unconventional sources stands poised to be a linchpin of a sustainable economy when coupled with cleaning of wastewater, hydrogen generation, and recovery of ancillary critical metals.

Keywords: Adsorption · Electrode fabrication · Electrochemical lithium extraction · Hybrid capacitive deionization · Insertion

Harris E. Kohl received his bachelor's degree in chemistry *magna cum laude* from Westminster College in New Wilmington, PA where he played varsity lacrosse and football. He is currently a PhD student under the advisement of Prof. Sarbajit Banerjee at Texas A&M University. He was awarded the National Science Foundation Graduate Research Fellowship in 2023.

Dr. Andrew Ezazi received his undergraduate degree from the University of Central Florida and a PhD in chemistry from Texas A&M University under the supervision of Prof. D. C. Powers developing new materials for solid state photochemistry applications. He then joined the laboratory of Prof. Sarbajit Banerjee as a postdoctoral research associate at Texas A&M University where he works on electrochemical direct lithium extraction using ζ-V_2O_5. Dr. Ezazi is also engaged in a startup venture translating work done in the Banerjee research group into products to enable the green energy transition. He has received several awards from Texas A&M to develop proof-of-concept prototypes.

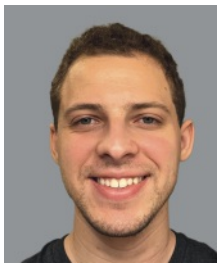

Carlos A. Larriuz, born in Toa Baja, Puerto Rico earned his BS in Chemistry from the University of Puerto Rico at Cayey in 2022. He is currently a PhD candidate and National Science Foundation-Alliances for Graduate Education and the Professorate (NSF-AGEP) fellow at Texas A&M University in Prof. Sarbajit Banerjee's research laboratory. His research focuses on electrochemical separation methods for direct lithium extraction using redox-active V_2O_5 insertion hosts in hybrid capacitive deionization.

Prof. Mohammed Al-Hashimi, FRSC, received his MSci honors degree in pharmaceutical chemistry in 2003 and his PhD in 2007 from Queen Mary University of London, UK. He was then a post-doctoral researcher at Imperial College London, UK. Al-Hashimi is a recipient of the Donald C. Bradley prize, the ASPIC prize, the Lefevre prize, the ACMME research prize, and the best research presentation award in Energy and Environment pillar ARC16. Dr. Al-Hashimi started his independent career at Texas A&M University at Qatar and is now a faculty member at Hamad Bin Khalifa University. He is best known for his work in designing and synthesizing organic polymers for electrochemical and optoelectronic applications.

*Correspondence: Dr. S. Banerjee, E-mail: sbanerje@ethz.ch
[a]Department of Chemistry, Texas A&M University, College Station, TX, 77843, USA; [b]College of Science and Engineering, Hamad Bin Khalifa University, P.O. Box: 34110, Doha, Qatar; [c]Laboratory for Inorganic Chemistry, Department of Chemistry and Applied Biosciences, ETH Zurich, Zurich, CH-8092, Switzerland; [d]Laboratory for Battery Science, Paul Scherrer Institute, Forschungsstrasse 111, CH-5232 Villigen PSI, Switzerland.

Prof. Hassan S. Bazzi, ACSF, FRSC, is the associate dean for external affairs, head of the division of science, and Full Professor of Chemistry at Hamad Bin Khalifa University. Between his graduate and post doctorial education at McGill University, Bazzi was awarded the Shield of H.E. President Emile Lahoud of Lebanon for his work in chemical weapons testing with the United Nations. Dr. Bazzi started his independent career at Texas A&M University Qatar where he won two Dean Leadership Awards (2012 and 2018) and a Dean Achievement Award (2014) for his outstanding service to the university. His studies focus on polymer chemistry, catalysis, and metathesis chemistry.

Prof. Sarbajit Banerjee, FRSC, FInstP, is a full Professor of Battery Materials in the Department of Chemistry and Applied Biosciences at ETH Zurich and serves as Head of the Laboratory for Battery Science at the Paul Scherrer Institute. Prior to starting at ETH and PSI in December of 2024, he was the Davidson Chair in Science and a Professor of Chemistry and of Materials Science & Engineering at Texas A&M University. He started his independent career at the University at Buffalo in 2007. His research interests are focused on energy storage, energy-efficient computation, metastable materials, and the development of synchrotron methods.

1. A Modern-Day Rush for White Gold

Challenges with scaling of energy storage represent a critical impediment to the energy transition. Battery energy storage technologies have a key role to play in expanding dispatchable clean-energy capacity in power grids, enabling grid firming, enhancing grid reliability, powering behind-the-meter load management, and for more efficacious transmission and distribution management.[1,2] In parallel, electrification of transportation fleets, spanning the range from forklifts to passenger electric vehicles, off-road vehicles, and electric aviation represents a critical thread in the decarbonization of transportation and global supply chains.[3] Improvements in performance, pathways to manufacturing at scale, and steep reductions in price/unit-energy stored are urgently needed for *intra*- and *inter*-day long-duration energy storage technologies, as well as for fleet electrification. As the most mature and versatile electrochemical energy storage technology at this point in history, lithium-ion batteries have a critical role to play in the energy transition.[4–6] However, the increasing emphasis on large-format batteries has stressed global supply chains for lithium and other critical materials such as cobalt, nickel, and graphite.[7-10] Demand for lithium is projected to skyrocket in the next three decades – approaching 6 million metric tons (Mmt) per year – a 25× increase from current production of *ca.* 0.24 Mmt.[11] It is estimated that by 2050 as much as 1.6 Mmt will be required for electric vehicles alone. Lithium, usually as lithium carbonate or lithium hydroxide, is currently sourced at scale by either mining or evaporation of brines.[12] These traditional production sources provide nearly all currently available lithium supplies but cannot guarantee future supply needs; mines on average take 10 years to reach full production capacity, evaporation pools can take up to 2 years.[13–15] These challenges in natural resource utilization have been exacerbated by geopolitical tensions, setting the stage for fierce competition for perhaps the most critical of limited mineral resources required for the energy transition.

Fig. 1 summarizes notable lithium deposits across the world and their form. Insets to Fig. 1 further list the leading producers and refiners of lithium. As a result of the large capital investments

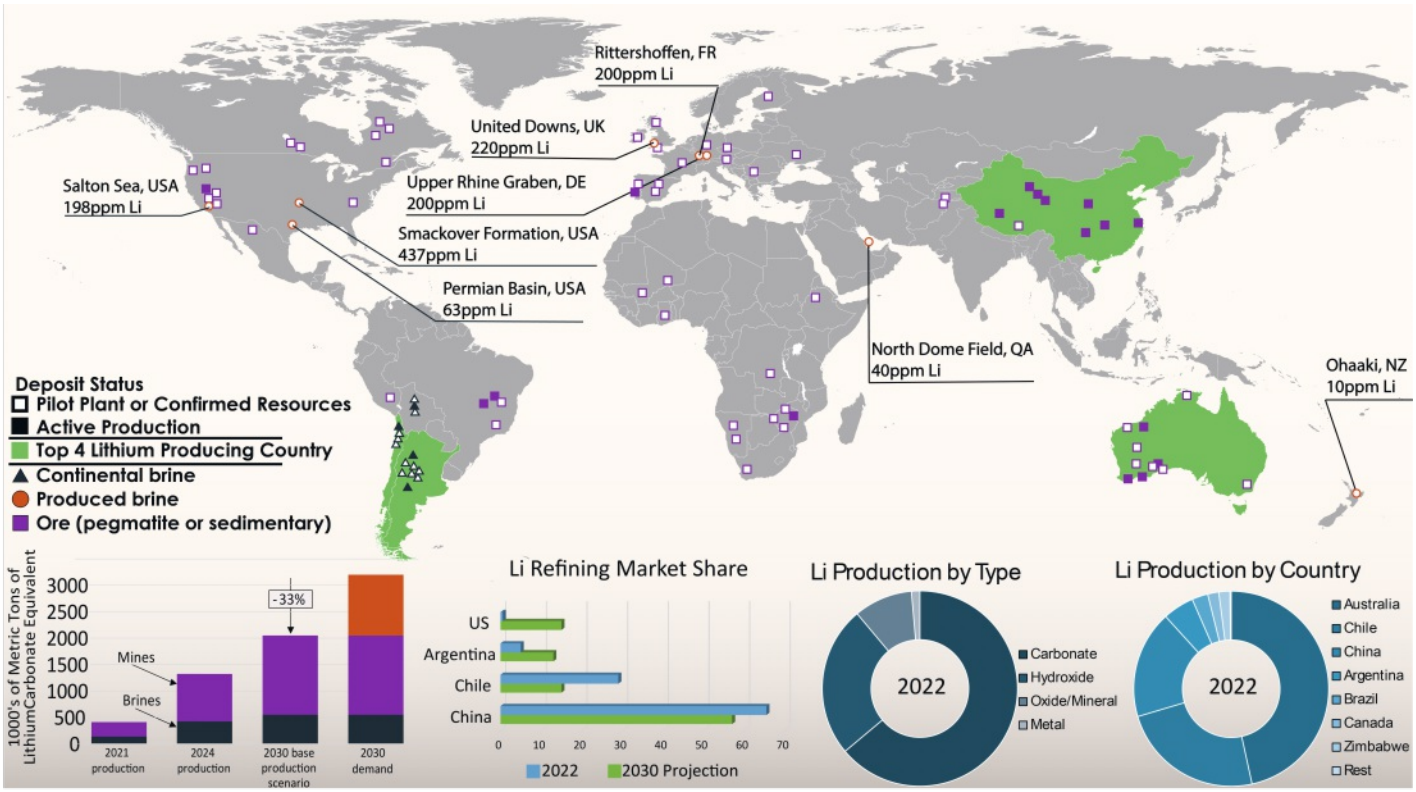

Fig. 1. Global map of lithium deposits mapping types of lithium source and indicating primary producers and refiners of lithium.[20] The bottom left inset shows projected lithium production and shortfalls for 2030.[11] The second-to-left inset shows lithium refining market share from three of the top producing countries along with future projections. The second-to-right inset shows lithium production by end-type.[18] The bottom right inset shows lithium production share by country.[18]

required, production capacities of mining and evaporation cannot be easily scaled to meet fluctuating demand. Indeed, lithium carbonate and hydroxide spot prices in China, the largest consumer of lithium for batteries, decreased dramatically in 2023.[16] The sluggish demand has forced production cuts and curtailed expansion and initiation of large-scale projects, which reflects in part the vagaries of price fluctuations and vulnerabilities of material supply chains to which many clean energy technologies are held hostage.[17] Despite current downward trends, the lithium market is still projected to grow well into the 2050's, with the supply-demand curve inverting around the turn of the decade.[18] Several analysts predict: (1) without new projects, known lithium deposits will likely be depleted by 2030, strangulating the energy transition; and (2) as a result of the exponential growth of the electric vehicle market and the time lag between the need for materials and the availability of end-of-life materials, battery recycling will have minimal impact on cumulative material demand for lithium in the near term.[8,9,11,19] The current trend in prices depressing or delaying new planned projects, combined with projections of massive demand, can potentially result in major supply chain challenges in the not-too-distant future. Thus, the need to develop and produce new sources of lithium rapidly and to advance technologies to extract lithium from unconventional dilute sources is dire.

Amongst the available sources of lithium, geothermal and oilfield-based brines have been at the forefront of the lithium expansion race.[21,22] These sources, which may range from the 10's of ppm to several thousand ppm in Li, have the potential to act as *pro tem* lithium sources, diversify supply chains, and potentially diminish the environmental impact and carbon footprint of large mining projects. The bottom inset to Fig. 1 shows that much of the anticipated gap in lithium supply is expected to be met from direct lithium extraction (DLE).[23–26] Currently, production methods for Li_2CO_3 can range in cost between $2-$9 USD per kg produced. Current cost estimates for pilot scale electrochemical DLE are already around $5 USD per kg, making electrochemical DLE a cost competitive approach; these prices are anticipated to drop sharply at scale as the levelized cost of clean energy plummets, technologies reliant on earth-abundant and inexpensive materials become available, and operational efficiencies are engineered across the process flow.[27]

The key problem to brine mining lies in efficient treatment and viable extraction of lithium from sources such as produced and flowback water generated in oil and gas operations. Produced water sources are often hypersaline and contain a plethora of contaminants: rock detritus, dissolved organic carbon, remnant hydrocarbons, and large concentrations of dissolved salts and mineral particles.[28] Treatment trains to reduce silt, sediment, and organic contaminants are commonplace and relatively inexpensive. However, discriminative treatment to reduce salinity or selectively extract lithium represents a formidable challenge.[29,30] Such workflows require orchestration of a complex sequence of energy-intensive steps. Selective removal of just lithium ions could dramatically reduce the cost and complexity of lithium extraction. The umbrella of burgeoning technologies focused on selective extraction of lithium is known as Direct Lithium Extraction (DLE).[31]

DLE technologies include adsorption, ion exchange, solvent extraction, and electrochemical methods.[30] Adsorption and ion-exchange technologies are currently the most advanced in the DLE space, usually being repurposed membranes. These membranes feature reasonable lithium selectivity and capacity but require regeneration to release lithium and begin a new cycle. Solvent extraction relies on coordination of lithium with an extracting agent, followed subsequently by phase transfer into a solvent that is immiscible with water. These processes also require large amounts of solvent and coordinating agents, and often struggle with throughput. Finally, electrochemical techniques represent a promising frontier for DLE.[29] These methods afford an excellent combination of selectivity and capacity; perhaps the greatest utility of these methods arise from the promise of coupling with inexpensive renewable power, such as solar, wind, or geothermal, in proximity to the extraction location, and from simplification of treatment trains, which obviates the need for large amounts of solvent and chemical additives.

2. Electrified Lithium Recovery

Electrochemical techniques for desalination and DLE can be generally categorized as Capacitive Deionization (CDI) and Hybrid Capacitive Deionization (HCDI). CDI and HCDI both operate using a similar device construct as exemplified in Fig. 2. A potential is applied between two high-surface-area electrodes and aqueous media with dissolved ions flow through a thin spacer layer. Alternative constructs involve liquid flow through porous electrified membranes or flowing parallel streams of particle slurries separated by membranes from the flow stream and held at different voltages. A key distinction between CDI and HCDI arises from the mode of ion sequestration, which is governed by the choice of material used to construct the active electrode. CDI is an electrosorption method wherein oppositely charged ions are adsorbed in proximity of the Stern layer extending out to the Debye length of the porous electrode architecture. Ion sequestration is achieved through a combination of specific adsorption onto (typically) activated carbons and oppositely charged ions attracted and bound within the diffuse layer.

In contrast, HCDI uses redox-active insertion hosts wherein electrosorption is followed by desolvation and ion-insertion into interstitial sites of the active material, which allows for storage of ions through the entire electrode volume (not just at surfaces) and imbues mechanisms for selective gating. Fig. 2 sketches a typical HCDI configuration and illustrates the need for thick high-surface-area porous electrodes that permit facile permeation of flow streams from which Li-ions can be sequestered and released through reversal of polarity. Fig. 3 shows mechanisms of electrosorption involving capacitive storage in the diffuse layer, pseudocapacitive storage involving specific surface redox, and desolvation and ion insertion, exemplified for a ζ-V_2O_5 insertion host (*vide infra*). Faradaic pseudocapacitive effects occur at particle surfaces as a result of surface redox events; such extrinsic pseudocapacitance does not require complete desolvation and thus affords a means of fast storage and release of ions. Notably, since such ions are adsorbed to the surface through redox reactions, the electrical double layer remains available to store an additional complement of ions.[32] In some cases, ion insertion can trigger phase transformations propagating to varying extents through the active particles.[5,33–35]

2.1 *Rating Ions Traps*

Fig. 2 shows the configuration of a DLE cell where the reservoir contains a dilute solution pre-treated to remove silt and sediment; in the case of some brines and most produced water, the input stream would have been subjected to other coagulation or nanofiltration approaches to reduce salinity or eliminate divalent cations.[28] The solution is then transported from the reservoir to the HCDI cell using a peristaltic pump. An HCDI cell typically pairs an insertion electrode with a high-surface-area carbon anode separated by an exchange membrane and separator. A voltage source creates a potential difference between these two electrodes (a reference electrode is used to prevent drift). Ions are captured and released in periodic cycles, thereby yielding enriched and depleted streams. Depleted streams can be recirculated to enhance Li-ion recovery.

Two measurements are commonly performed, a conductivity measurement in the reservoir and chronoamperometry or chronocoulometry in the HCDI cell depending on constant-voltage or

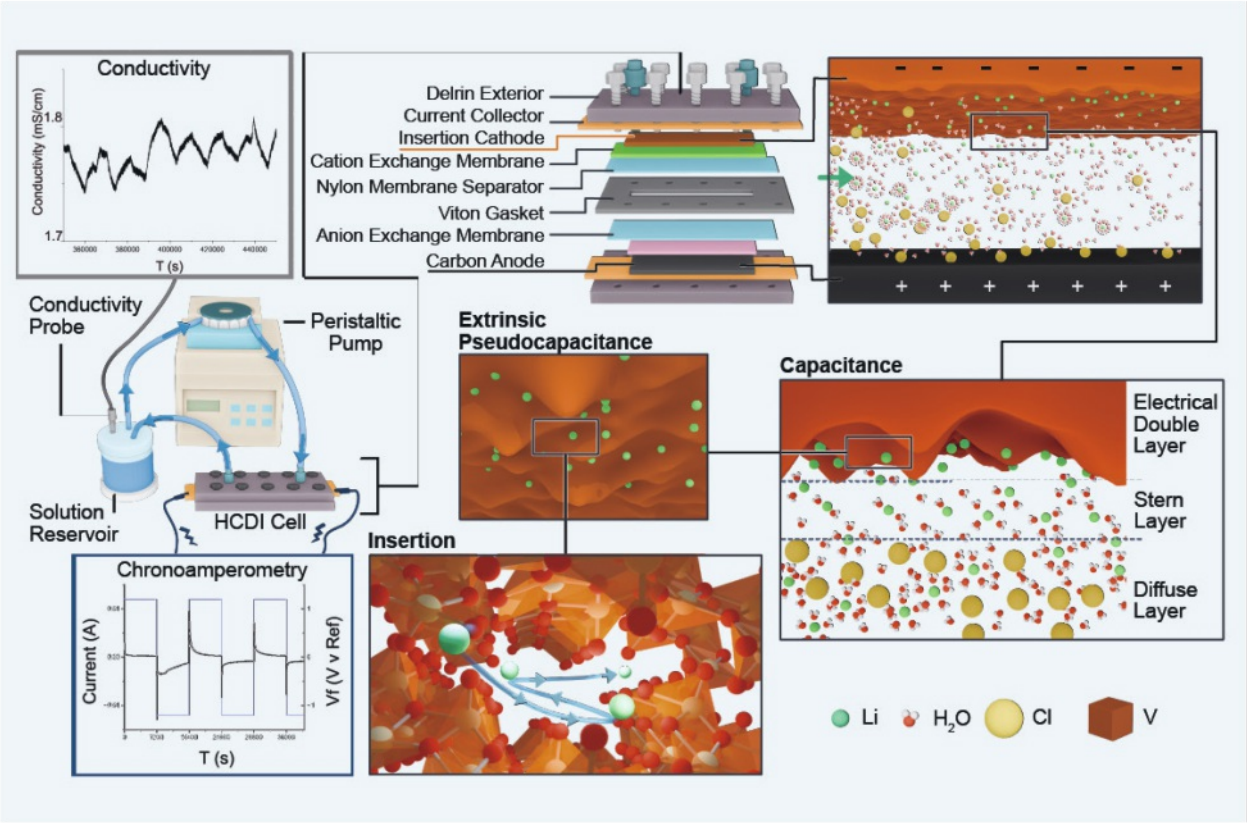

Fig. 2. In a typical HCDI cell illustrated here, conductivity is measured in the solution reservoir, whereas chronoamperometry is performed within the HCDI cell. Different modes of ion sequestration are illustrated from the surface electrical double layer to insertion into the bulk. Three distinct modes of ion sequestration are shown: the electrical double layer, extrinsic pseudocapacitance, and insertion.

constant current operation. The former provides a measure of ion concentration in the reservoir, whereas the electrochemical measurement provides a measure of evolution of ion current or electrode potential difference in response to ions entering the insertion electrode.[36] These measurements are crucial for effective understanding of HCDI and for evaluating its efficacy, selectivity, and robustness in DLE. Some key metrics to judge the relative efficacies of processes, cell configurations, and active electrodes include the Desalination Capacity, which is a metric of the number of ions effectively sequestered as per:

$$Desalination\ capacity = \frac{\nu M_{LiX}}{m_{total}} \int C\, dt \ldots \quad (1)$$

where ν is the flowrate ($L \cdot s^{-1}$), M is the molecular weight of the LiX salt (X represents the counter-ion), m is the mass of both

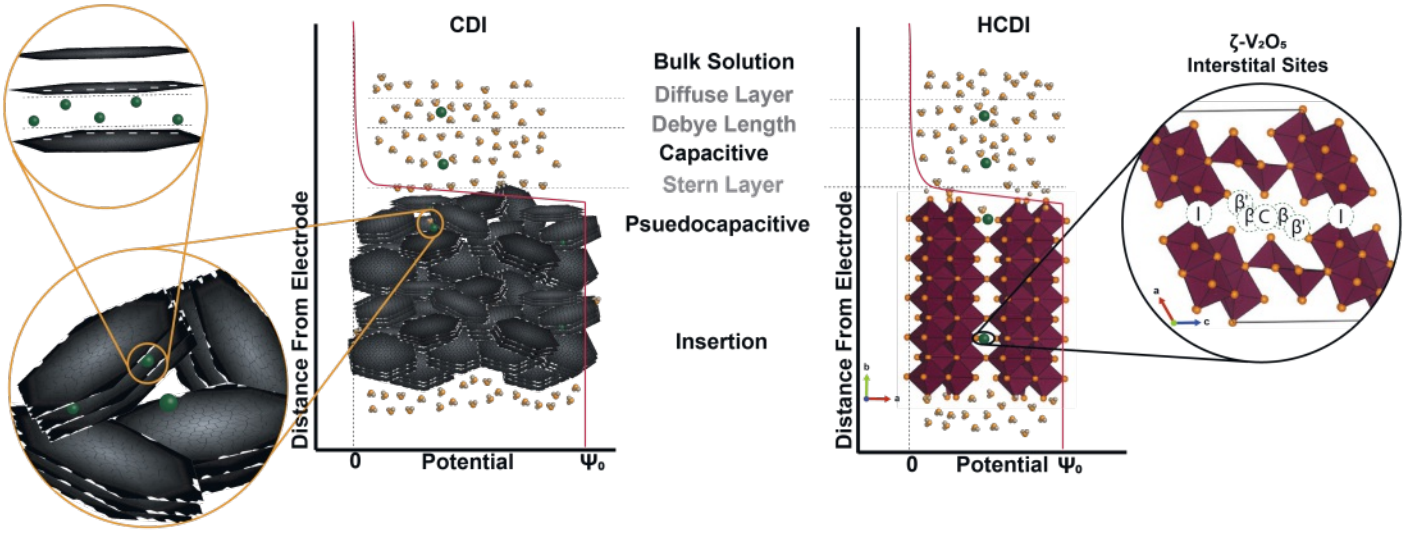

Fig. 3. Ion capture events in CDI *vs*. HCDI. CDI utilizes activated high-surface-area electrodes to store ions in the electrical double layer (EDL) and in pseudocapacitive sites depicted on the left of the figure. The HCDI host electrode, however, has an additional form of adsorption. Here after the pseudocapacitive sites have been saturated the lithium-ion is desolvated and inserted into interstitial sites within the host electrode. These sites are depicted to the right of the figure for ζ-V_2O_5 as an insertion host of particular emphasis in this work.

electrodes in the system, and $\int C\,dt$ is the integrated area under the concentration-time curve for each half cycle, units in mmol L^{-1}s. Another important metric is specific Ion Removal Capacity (IRC). This can be used to evaluate the amount of a specific ion that is being extracted from the system. The key input and cost in electrochemical lithium recovery is power. In addition to metrics accounting for the mass of ions extracted from flow streams, the amount of energy is a critical consideration and is represented by the Charge Efficiency (CE), exemplified again for LiCl as:

$$CE(\%) = \frac{\frac{Desalination\ Capacity}{M_{LiCl}}}{\frac{Q}{F}} \times 100\% \ldots \quad (2)$$

$$\text{where } Q = \frac{q}{m_{total}} \ldots \quad (3)$$

where F is Faraday's constant and Q is the average total charge stored in both electrodes normalized to the total mass of both electrodes, q is the amount of charge passed through the system, calculated by integrating the chronoamperometry data of each charging half cycle. The CE provides a measure of the efficacy of insertion reactions as compared to parasitic reactions such as cathode dissolution and interphase formation. The closer this number is to unity, the greater the preference for desolvation and insertion processes as compared to unproductive parasitic reactions.

A factor of critical importance to electrochemical lithium extraction is selectivity. Most often, unconventional sources have higher concentrations of other monovalent and divalent cations than lithium, making it imperative to have high degrees of lithium selectivity. Selectivity is calculated as per:

$$\beta_{\frac{A}{B}} = \left(\frac{DC_A}{DC_B}\right)\left(\frac{C_{B,feed}}{C_{A,\,feed}}\right) \ldots \quad (4)$$

where $\beta_{\frac{A}{B}}$ is the unitless separation factor for two different ions A and B, DC_A and DC_B are the desalination capacities of each ion respectively, gathered from measurements such as inductively coupled plasma mass spectrometry or ion chromatography, and $C_{A,\,feed}$ and $C_{B,\,feed}$ are the concentrations of the two ions in the original solution. There are often trade-offs between quantities such as IRC and selectivity; for instance, mechanisms dominated by capacitive or supercapacitive processes augment ion sequestration but are much less discriminating towards Li-ions. Other relevant metrics pertain to kinetics of ion removal and release cycles and cycle life, which reflects the resilience of the active material and porous electrode architecture from common degradation mechanisms such as chemo-mechanical failure, surface passivation, carbon corrosion, or cathode dissolution.

2.2 *Navigating Multidimensional Process Design Spaces*

DLE metrics depend not just on material considerations but also on the specifics of the cell configuration (Fig. 2), as well as process considerations such as applied potential, flow rates, temperature, and cycle times. Judicious consideration of cell and process parameters can be used to promote reversible ion sequestration and alleviate deleterious parasitic reactions such as carbon corrosion and water splitting.[37,38] Local entrapment of gaseous bubbles can impede electrolyte diffusion to the surfaces of the active insertion electrode and thereby reduce the efficacy of electrochemical lithium extraction. Another process consideration that is noteworthy is the mass balance between the two electrodes. In HCDI, the two electrodes can be starkly different in their ion uptake given the distinctive processes operational at the insertion cathode and the carbon anode as illustrated in Fig. 3. Optimizing the mass ratio between the insertion electrode and the carbon anode helps expand the voltage window available for the insertion electrode.[39]

Temperature is a process parameter of particular importance to geothermal brines; a detailed understanding of temperature-dependence of DLE metrics and of the robustness of HCDI components is imperative to determine the optimal integration of HCDI cells *vis-à-vis* heat exchangers used in geothermal plants.[40,41] Considering $LiFePO_4$, an intriguing tradeoff is observed between accessible capacity and capacity retention; at lower temperatures, the initial capacity is low, but capacity retention is improved as compared to higher temperatures.[42] The results reflect the relative thermal activation of insertion reactions as compared to parasitic reactions such as interphase formation and cathode dissolution. Another set of important process parameters relates to the mode of operation, under constant current or constant potential.[43]

Given the vast design space of geometric configurations and process conditions, HCDI methods will benefit from a systematic design-of-experiments approach aided by machine learning methods to efficiently navigate across the design space of operational conditions. As an example of such an approach, a Box-Behnken design of experiments can be used to survey the design space and build models that relate electrode and flow reactor geometry, flow rate, and measured characteristics to ion-removal capacity and kinetics.[44] AI/ML iterative frameworks can be subsequently used to navigate multi-dimensional design and operational spaces and identify features that optimize across a Pareto frontier of ion-removal capacity, kinetics, selectivity, and cyclability.[44-46]

2.3 *Designing Across Length Scales to Enable Effective Electrochemical Lithium Extraction*

Fig. 4 sketches the structures of insertion hosts used in HCDI, which have a high concentration of interstitial sites available for lithium sequestration along with redox-active transition metal centers.[40,47–49] These are familiar battery positive electrode materials, which must meet additional constraints of stability in aqueous media and under modest excursions from neutral pH. A key aspect that distinguishes insertion phenomena in HCDI from conventional weakly coordinating electrolytes is the challenge of desolvating tightly bound water molecules at the electrified interface. 'Hard' Li-ions have a large hydrated ionic radius, which along with their high hydration free energy of as much as 515–544 kJ/mol, pose a much greater barrier to desolvation at electrified interfaces as compared to Li-ion desolvation from non-aqueous electrolytes encountered in battery electrode materials.[50] Insertion of Li-ions is driven by Faradaic redox processes and generally induces an expansion of the lattice.[51] In some instances, ion insertion beyond a certain concentration drives phase transformations that open up an additional complement of interstitial sites for accommodating Li-ions. Additional challenges result from: i) competitive insertion of protons at hydroxylated interfaces;[52,53] ii) parasitic reactions activated at relatively modest excursions from neutral pH including deleterious interphase-forming reactions, surface dissolution, and coupled water/oxygen redox that can result in surface corrosion;[53,54] and iii) capillary forces resulting from the high surface tension of water that can induce local dewetting or exacerbate chemo-mechanical degradation of interphasic layers. Mitigating these challenges requires materials design spanning from atomistic site-selective modifications to choice of crystal lattice or framework, particle geometry, and 3D mesoscale electrode structure[5] (Fig. 2).

The electrochemically active insertion hosts are typically insulating in nature. Typically, a conductive additive such as carbon and an inactive binder such as poly(vinylidene difluoride) (PVDF) are mixed in a solvent such as *N*-methyl-2-pyrrolidone (NMP) to form a slurry, which is used to cast conformal thin film porous electrodes on current collectors (recent interest has focused on dry mixing processes to eliminate use of NMP). Given that the PVDF

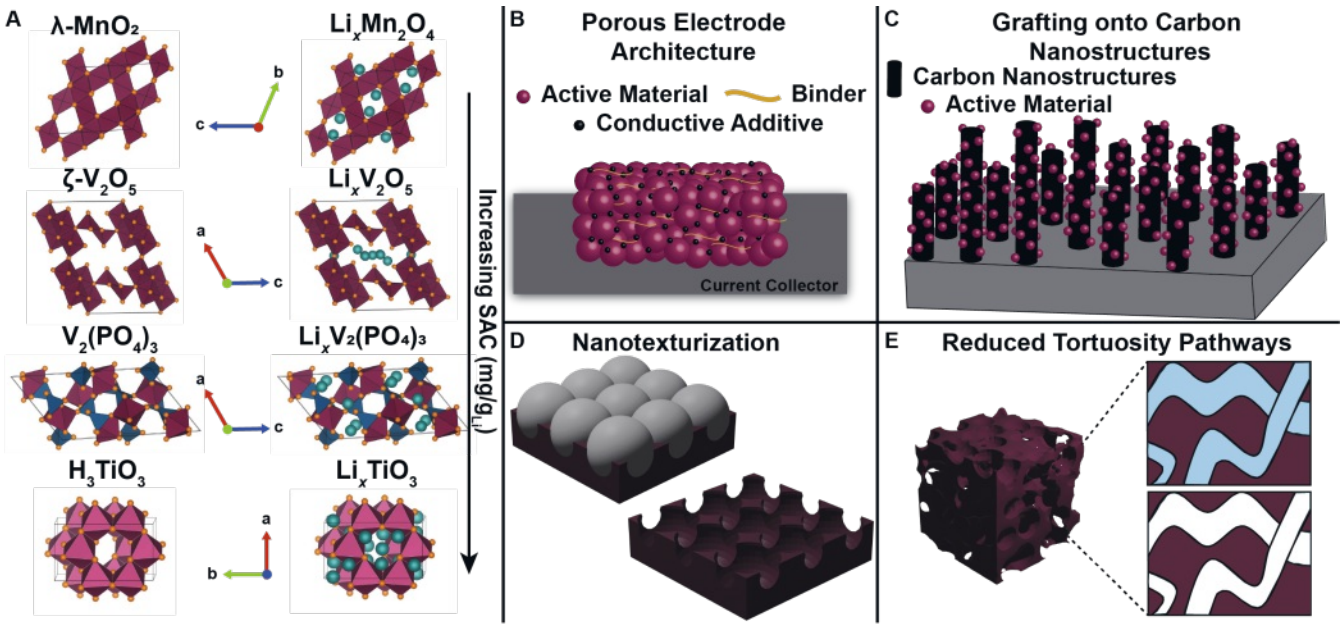

Fig. 4. A) Illustrative examples of insertion electrode materials empty (left) filled (right); B) Typical porous electrode architectures fabricated from slurries; C) Grafting active material onto carbon nanostructures to increase conductivity; D) Nanotexturization using templates such as block copolymers has shown to increase electrochemical activity by allowing more surface exposed tunnels; E) Engineering multiscale porosity to improve electrode wettability and reduce tortuosity of ion diffusion pathways in HCDI.

and carbon have a limited ability to sequester ions, much interest has focused on electrode fabrication processes that maximize the loading of the active material.

Design of the insertion host is a critical imperative but not entirely sufficient since overall performance also depends on control of the mesoscale porosity, which governs the effective tortuosity of ion diffusion pathways. The geometry of active cathode material particles and mode of particle aggregation determines the next length scale that governs different ion sequestration mechanisms.[5] Fig. 4B shows conventional porous electrode architectures where active electrode particles are mixed with a binder and conductive carbon. Fig. 4C and D illustrate different approaches to reduce tortuosity and enable effective utilization of thick electrodes.[55–57] In an alternative approach, insertion electrodes have been deposited onto arrays of carbon nanostructures using atomic layer deposition and sol-gel methods.[58–63] These methods are advantageous in affording optimal porosity, and as a result of the conductivity derived from carbon nanostructures; however, thin film electrodes sacrifice overall IRC at the cost of fast kinetics. Exposed carbon surfaces further degrade ion selectivity since they can only sequester ions through capacitive processes, thereby squandering the differentiated ion uptake resulting from insertion and solid-state diffusion of Li-ions in redox-active insertion hosts. Depending on the degree of lattice expansion induced by ion insertion and resulting phase transformations, stresses generated within individual particles can compound across length scales, resulting in electrode pulverization or delamination from the current collector.[34,57] Paramount considerations in the design of 3D electrode architectures are the alleviation of mass-transport limitations, ensuring homogeneous aqueous wettability, maintaining electrical contact for densely packed particles, and preservation of the electrode architecture upon prolonged cycling.

2.4 *A Case Study of Brine Mining from the Arid Permian Lands*

Produced waste water from oil and gas production in the Trans-Pecos Permian Basin of West Texas approaches volumes in excess of 19 million barrels per day.[65] Li content in this produced water varies geographically and temporally but averages in the high 10's to several hundred ppm.[28] We have sought to simultaneously implement DLE along with recovery of other high-value trace elements and cleaning of produced water with a view towards utilizing the abundance of solar and wind power in West Texas. Produced and flowback water in this region is hypersaline with a high content of silt particles, fracked hydrocarbons, and natural organic matter. We have designed a 3D hierarchically textured high-flux desilting and deoiling membrane based on calcium sulfoaluminate-cement and glass beads embedded onto a periodic metal mesh.[28,66–68] The membrane exhibits orthogonal wettability, specifically, a combination of super-hydrophilic and underwater superoleophobic characteristics, which enables effective removal of oil. Such membranes were shown to be highly effective in the removal of silt particles and oil droplets from produced water sourced from 13 different wells across the Delaware and Midland Basins of West Texas (Fig. 5) at record high flux rates (1600 $L \cdot h^{-1} \cdot m^{-2}$, at *ca.* 2.7 bar). Single-pass deoiling is achieved down to 1 ppb, with removal of >99% of silt particles, as illustrated in Fig. 5C.[28]

Next, we have devised an electrochemical DLE method based on the distinctive 1D tunnel-structured ζ-V_2O_5 insertion host shown in Figs. 3 and 5. Up to 10^3 selectivity for Li/Na and 10^4 selectivity for Li/Mg is achieved.[48] The porous electrode architectures retain their selectivity and preserve their integrity down to pH values of 5.0, and thus are compatible with a broad range of produced-water. The crystallographic sites where Li-ions are sequestered have been unambiguously identified, as illustrated in Fig. 3 paving the way for modification strategies to further improve selectivity, IRC, and kinetics.[69]

3. Materials Design for HCDI

Improving the performance of HCDI systems for selectively extracting target ions relies on modifying cathode materials to enhance selectivity, diffusivity, and removal capacity. Such strategies are nascent for electrochemical lithium extraction but can take a leaf from the expanding playbook becoming available for tuning insertion electrodes for aqueous batteries, multivalent ions, and tailored cathode electrolyte interphase formation. Such studies are providing growing insight into desolvation and interfacial

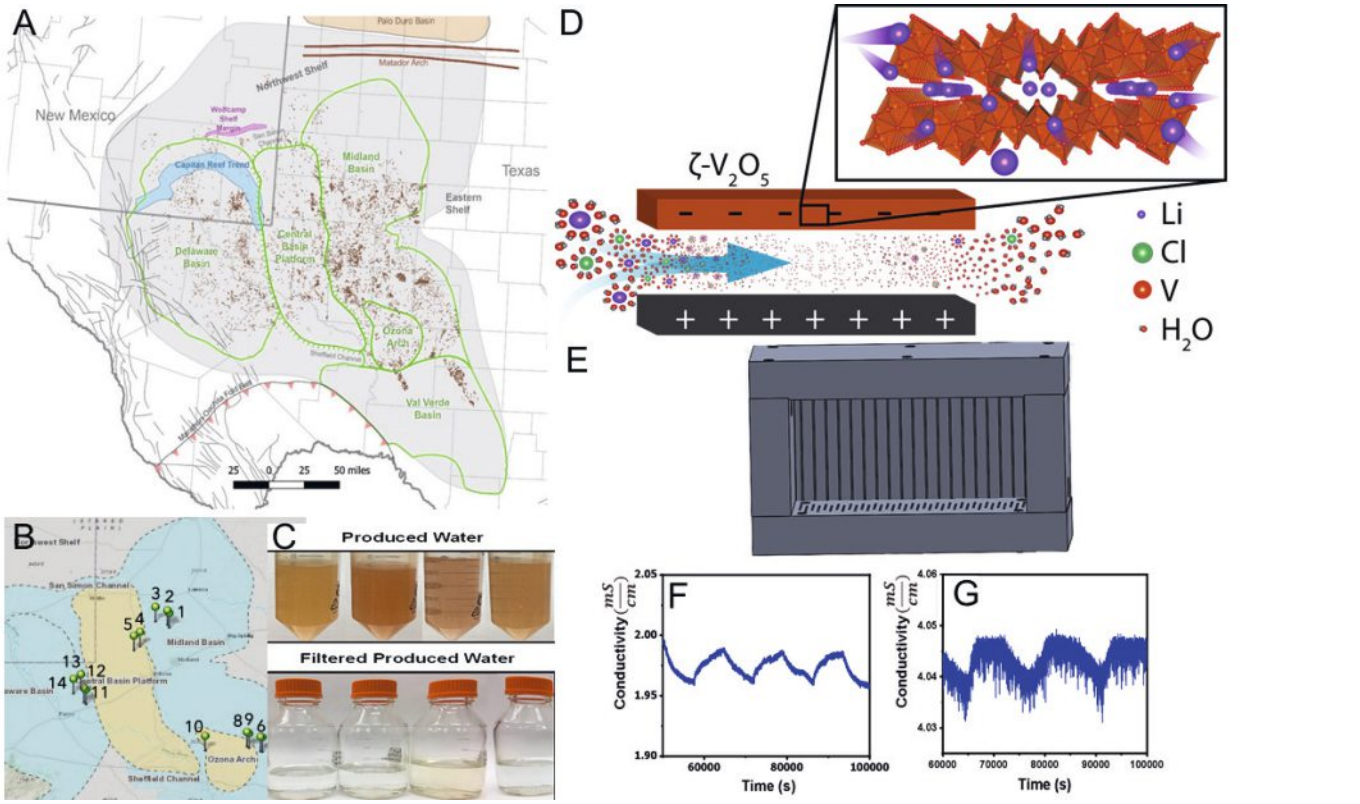

Fig. 5. A) Map of Permian Basin illustrating geographic figures and well locations. Reprinted from U.S. Energy Information Administration, Permian Basin, Part 2 (March 2022); B) Map of well locations where produced water has been sampled.[64] Reprinted with permission from ref. [2]; C) Cleaning of produced water using CSA/glass-bead 3D porous membrane integrated onto metal mesh. Reprinted with permission under CC 4.0 license from ref. [28]; D) Schematic illustration of HCDI configuration utilizing a ζ-V_2O_5 cathode. Reprinted with permission from ref. [48]; Copyright 2022 American Chemical Society. E) Rendering of a nominal bench scale flow-through benchtop prototype; F) Ionic conductivity versus time plot for a flowstream containing a 15 mM aqueous solution of LiCl. Reprinted with permission from ref. [48]; Copyright 2022 American Chemical Society. G) Conductivity *vs.* Time plot for produced water samples. The produced water stream is pre-treated by filtration through the CSA module before being flowed across the HCDI cell. Reprinted with permission from ref. [48]. Copyright 2022 American Chemical Society.

chemistry at electrified interfaces; sequence of interstitial sites occupied; diffusion pathways traversed by ions; evolution of atomistic structure, crystal lattice, and mesoscale porosity with ion insertion/extraction; and the coupling of electrochemistry with particle and electrode geometry (Fig. 6).[51,70–74] We discuss here some strategies with specific reference to V_2O_5 as an insertion host for HCDI but with broad generalizability to other insertion electrode materials such as shown in Fig. 7. Key strategies include choice of structure-type or site-selective modification, as well as mesoscale optimization of electrode architecture to help with electrolyte accessibility for improved Li-ion extraction performance. Fig. 6 depicts a range of these modifications that can be accomplished to enable specific enhancement of DLE metrics and alleviate common degradation mechanisms noted in preceding sections.

Considering the rugged energy landscape of V_2O_5 polymorphs, single-layered α-V_2O_5 represents the thermodynamic minimum.[5,70] The α-V_2O_5 phase undergoes a series of phase transformations as a function of increasing Li-ion insertion.[3–5,20–23] For low concentrations of Li-ions, the thermodynamically stable α-V_2O_5 generally retains its structure with some expansion of interlayer spacing and canting of vandyl moieties to coordinate to Li-ions in interlayer sites. Further concentrations ($0.33 \leq x \leq 0.80$) lead to additional puckering of the vanadyl bond and give rise to the ε-$Li_xV_2O_5$ phase, which retains the *Pmmn* space group. As the lithium concentration increases ($0.80 \leq x \leq 1.00$) in this system, the δ-$Li_xV_2O_5$ phase is stabilized in the *Ammn* space group. Beyond stoichiometries of one Li-ion per V_2O_5, puckering as well as rotations of the [VO_5] units are observed, which give rise to an irreversible transformation to the

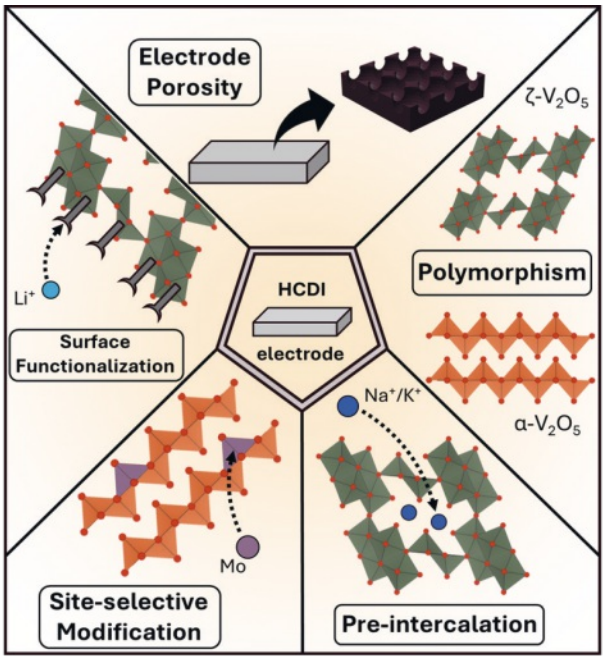

Fig. 6. Illustration of strategies used for enhancing the capacity and selectivity of redox-active hosts in HCDI categorized by different length scales. The strategies are presented in a clockwise progression, starting with electrode-scale optimizations, such as porosity, and moving through the *meso*- and *atomistic*-scale methods, which include polymorphism, pre-intercalation, site-selective modification, and surface functionalization.

puckered single-layered γ-$Li_xV_2O_5$ ($1.00 \leq x \leq 2.00$) and rock-salt disordered ω-$Li_xV_2O_5$ ($2.00 \leq x$) phases.[70,75–77] When α-V_2O_5 is used as an HCDI electrode, capacity is diminished within a few cycles as a result of irreversible phase transformations during lithiation and electrode pulverization as a consequence of stress buildup from volumetric changes associated with phase inhomogeneity (Fig. 6).[75]

One approach to alleviate the phase transformations relies on modification of thermodynamics of the phase transformations and improving the congruency of the two lattices. In past work, we have shown that site-selective substitution of Mo onto V sublattices of α-V_2O_5 yields extended single-phase regimes. Mo-alloying induces pre-transformations that modify the α-V_2O_5 crystal structure and render the lithiation-induced phase transformations less abrupt in their changes of order parameters. Two notable consequences include: (i) extended solid-solution lithiation regimes without phase transformation; and (ii) rendering phase transformations reversible across a broader range of lithiation.[78] Alternative strategies include surface functionalization either with molecular monolayers or conformal thin-film coatings. Molecular monolayers can potentially aid selective binding or pre-concentration of target ions and facilitate their desolvation (Fig. 6), whereas conformal monolayers can mitigate cathode dissolution, stabilize surface phase transformations, and provide conductive pathways to alleviate challenges to electronic and ion diffusion.[79,80]

Manganese oxides such as Na-birnessite and Mg-busserite, which have been extensively investigated for HCDI[81,82] show degradation of electrochemical performance after 200 cycles, which could perhaps be alleviated in part through electrode engineering to sequester dissolved Mn ions and provide a conformal coating to entirely prevent Mn dissolution.[79,81,83] As an alternative to storing ions within interstitial sites, structural defects such as cation vacancies can further serve as ion reservoirs. For example, $ZnMg_2O_4$ spinel and $Na_2FeP_2O_7$ have shown promise for electrochemical sequestration of Zn^{2+} and Na^+ in generated vacancies, highlighting their potential or selective ion extraction in HCDI.[84,85]

As sketched in Fig. 4, when considering strategies to improve efficiency of electrochemical Li-ion extraction, mesoscale texture and porosity of porous electrodes further need to be designed to enable effective utilization of thick electrodes at viable cycling rates. Approaches to reduce tortuosity of diffusion pathways need to be combined with atomistic design and site-selective modifications strategies to maximize the performance of the active material in HCDI electrodes.

Effects of parameters such as electrode thickness have been previously evaluated in manganese oxide systems used in HCDI.[86] Key findings indicate an increase in salt removal capacity for cathode thicknesses up to at 450 μm. Conversely, increasing the thickness to 600 μm results in a significant decrease in removal performance.[86] Fig. 4B shows various strategies for introduction of porosity such as through engineered channels or use of templates to impart mesoscale porosity. For instance, spinel lithium iron manganese oxides have been templated to stabilize micropores that enable full wettability of the material, which in turn increases effective ion transport and, consequently, leading to an improved salt/ion removal capacity.[43] The introduction of multiscale porosity and engineered channels not only helps mitigate stress effects caused by phase heterogeneity within the electrodes, thereby ensuring preservation of the electrode architecture, but also influences greatly enhanced ion diffusion rates, which is critical to obtain rapid sequestration and release cycles. As such, electrode design across decades of length scales is necessary to obtain optimal parameters for electrochemical Li-ion recovery navigating complex trade-offs along Pareto frontiers.

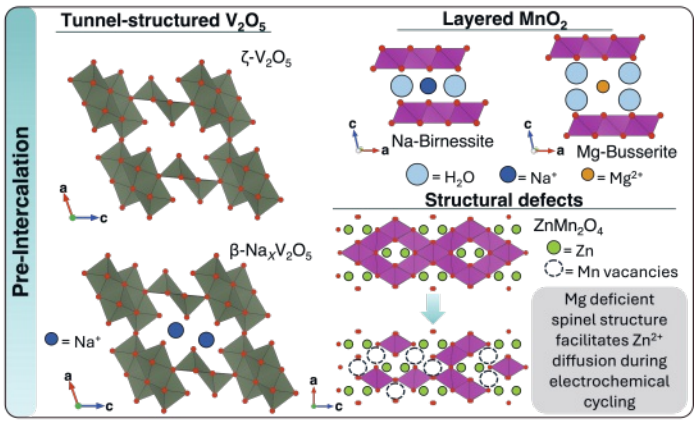

Fig. 7. Illustration of various crystal structures demonstrating the effects of pre-intercalation on enhancing selectivity and capacity in HCDI systems. The left panel shows pre-insertion of the tunnel structured ζ-V_2O_5 with Na-ions to yield β-$Na_xV_2O_5$. The right panel shows pre-intercalated layered MnO_2 compounds with stabilizing ions such as Na- and Mg-ions (top) and a spinel MnO_2 where Mn vacancies within the structure favor Zn-ion sequestration (bottom).

4. Sector Coupling

Electrochemical lithium recovery holds promise for being the linchpin for an interconnected system of circularity and clean energy technologies (Fig. 8). In the case of geothermal brines, Li-ion recovery modules can be coupled to heat exchangers to enable simultaneous harvesting of subsurface geothermal energy. For oil field and gas field brines, the removal of silt and oil, such as illustrated in Fig. 8, represents a potential path towards reducing costs of disposal of wastewater. HCDI technologies offer an efficient alternative to conventional desalination methods like reverse osmosis and electrodialysis.[87,88] HCDI consumes less energy and is more tolerant of salinity levels, which makes it a particularly useful choice for hypersaline water.[8] In contrast, RO requires high pressure to force water through membranes, which incurs substantial energy consumption.[87] Indeed, HCDI-based treatment trains can embed additional valorization modules, such as for the recovery of transition metals and rare-earths using membrane-based systems or specially designed electrochemical flow cells. Specific modules can enable isotope enrichment or removal of radioactive isotopes. While electrodialysis is generally more energy-efficient for bulk desalination, HCDI's ability to target and recover specific high-value ions, along with its operational flexibility, makes it a powerful and versatile option for producing potable water and advancing resource recovery.[82,86,88] Given the geographic spread of oilwells and the nature of drilling operations in West Texas, a modular truck as sketched in Fig. 8 is likely the most economically viable alternative that will mitigate the need to transport large volumes of water across long distances. After lithium sequestration, precipitation can be initiated in an enriched stream by addition of sodium carbonate or *via* atmospheric plasma processes. Both options would yield lithium carbonate, a primary ingredient in battery manufacturing.

5. Conclusions

HCDI has demonstrated the potential to bridge the gap between future lithium demand and supply based on electrochemical extraction of lithium from existing processes that produce low-concentration effluent streams such as geothermal brines and produced water. Viable lithium extraction requires enhancing the selectivity, capacity, and kinetics of lithium-ion insertion in insertion electrodes that serve as the active elements of HCDI cells. Viability of electrochemical lithium extraction is predicated on metrics such as ion removal capacity, charge efficiency, and selectivity, which requires optimal design of cell configuration,

Fig. 8. Sector coupling related to HCDI operations. Mounted truck operations provide mobile solutions to produced water sources. Potential synergistic applications include isotope and transition metal recovery, water treatment, energy generation, and carbon capture.

process conditions, and materials design across length scales from atomistic to mesoscale dimensions. Effective lithium extraction at electrified interfaces requires promotion of selective ion sequestration over undesirable parasitic reactions such as corrosion and dissolution, fast desolvation kinetics, and selective insertion and extraction of Li-ions across a broad complement of interstitial sites throughout the volume of the insertion electrode. While full mechanistic understanding remains to be fully elucidated, we point to several emerging design principles for modulation of selective Li-ion uptake with fast kinetics based on site-selective substitution, pre-insertion, selection of particle geometry, and reduction of ion diffusion tortuosity. HCDI can be coupled with various processes such as negative emissions, hydrogen generation, desalination, and geothermal energy harvesting to improve economic viability. The use of inexpensive renewable energy and the facile recyclability of membranes, stacks, and active insertion hosts alike portends substantial improvements in price competitiveness of these technologies in the years to come. As such, HCDI stands poised to be a key linchpin for a sustainable and circular economy.

Acknowledgements

This work was funded by the Texas A&M System Translational Investment Fund. H.E.K acknowledges the support of the SNSF under a Graduate Research Fellowship grant DGE: 1746932. We acknowledge support from the Qatar Research, Development and Innovation Council, Qatar National Research Fund (ARG01-0522-230270).

Received: October 15, 2024

[1] K. Scott, S. Hendrickson, N. Ryan, A. Dawson, K. Kort, B. Shrager, V. Siberry, P. Spitsen, S. Babinec, P. Balducci, Z. Zhou, D. Crane, K. Cummins, M. Klenbara, V. Chan, L. Tian, J. Shah, J. Wagner, 'Pathways to Commercial Liftoff: Long Duration Energy Storage', Department of Energh, **2023**, https://liftoff.energy.gov/wp-content/uploads/2023/03/20230320-liftoff-LDES-vPUB.pdf.

[2] J. A. Dowling, K. Z. Rinaldi, T. H. Ruggles, S. J. Davis, M. Yuan, F. Tong, N. S. Lewis, K. Caldeira, *Joule* **2020**, *4*, 1907, https://doi.org/10.1016/j.joule.2020.07.007.

[3] A. Brucker, A. Duran, N. P. Sullivan, A. Mistry, *ACS Energy Lett*. **2024**, *9*, 4053, https://doi.org/10.1021/acsenergylett.4c01276.

[4] J. B. Goodenough, Y. Kim, *Chem. Mater*. **2010**, *22*, 587, https://doi.org/10.1021/cm901452z.

[5] D. A. Santos, S. Rezaei, D. Zhang, Y. Luo, B. Lin, A. R. Balakrishna, B.-X. Xu, S. Banerjee, *Chem. Sci*. **2023**, *14*, 458, https://doi.org/10.1039/D2SC04157J.

[6] M. S. Whittingham, *Nano Lett*. **2020**, *20*, 8435, https://doi.org/10.1021/acs.nanolett.0c04347.

[7] H. Hao, Y. Geng, J. E. Tate, F. Liu, K. Chen, X. Sun, Z. Liu, F. Zhao, *Nat. Commun*. **2019**, *10*, 5398, https://doi.org/10.1038/s41467-019-13400-1.

[8] C. Xu, Q. Dai, L. Gaines, M. Hu, A. Tukker, B. Steubing, *Commun. Mater.* **2020**, *1*, 99, https://doi.org/10.1038/s43246-020-00095-x.

[9] G. Harper, R. Sommerville, E. Kendrick, L. Driscoll, P. Slater, R. Stolkin, A. Walton, P. Christensen, O. Heidrich, S. Lambert, A. Abbott, K. Ryder, L. Gaines, P. Anderson, *Nature* **2019**, *575*, 75, https://doi.org/10.1038/s41586-019-1682-5.

[10] A. Zeng, W. Chen, K. D. Rasmussen, X. Zhu, M. Lundhaug, D. B. Müller, J. Tan, J. K. Keiding, L. Liu, T. Dai, A. Wang, G. Liu, *Nat. Commun*. **2022**, *13*, 1341, https://doi.org/10.1038/s41467-022-29022-z.

[11] M. B. Azevedo, M. Baczyńska, K. Hoffman, A. Krauze, McKinsey & Company *Metals & Mining*, **2022**, https://www.mckinsey.com/industries/metals-and-mining/our-insights/lithium-mining-how-new-production-technologies-could-fuel-the-global-ev-revolution.

[12] N. Zhou, H. Su, Q. Wu, S. Hu, D. Xu, D. Yang, J. Cheng, *Resources Policy* **2022**, *78*, 102866, https://doi.org/10.1016/j.resourpol.2022.102866.

[13] R. Krishnan, G. Gopan, *Clean. Eng. Technology* **2024**, *20*, 100749, https://doi.org/10.1016/j.clet.2024.100749.

[14] C. Clifford. 'The "land grab" for lithium is just getting started with GM deal', 15, says EV materials expert. CNBC, https://www.cnbc.com/2023/01/31/land-grab-for-lithium-is-just-getting-started-with-gm-expert-says.html#:~:text=%22EV%20companies%2C%20especially%20the%20auto,a%20lithium%20mine%2C%20Moores%20said.

[15] P. E. Xu, Gomes-Callus, Choi, Sung. 'Direct Lithium Extraction: Readiness assessment'. BloombergNEF, **2024**, https://about.bnef.com/blog/direct-lithium-extraction-on-the-cusp-of-commercialization/.

[16] B. W. Jaskula, U.S. Geological Survey Mineral Commodity Summaries - Lithium, **2024**, https://pubs.usgs.gov/periodicals/mcs2024/mcs2024-lithium.pdf.

[17] D. A. Santos, P. Pradeep Kumar, M. K. Dixit, S. Banerjee, *Matter*. **2021**, *4*, 4, https://doi.org/10.1016/j.matt.2020.12.009.

[18] 'Global Critical Minerals Outlook 2024'. International Energy Agency (IEA), **2024**.

[19] L. Gaines, *Sustain. Mater. Technologies* **2018**, *17*, e00068, https://doi.org/10.1016/j.susmat.2018.e00068.

[20] R. A. Shaw, British Geological Survey Commissioned Report, CR/22/123, 8pp, **2022**, https://ukcmic.org/downloads/reports/the-potential-for-lithium-in-the-uk-2022.pdf..

[21] A. V. Nagar, S. Ventura, S. Bhamidi, M. Hornbostel, California Energy Commission, **2024**, CEC-500-2024-020, https://www.enery.ca.gov/publications/2024/pilot-scale-recovery-lithium-geothermal-brines.

[22] I. Warren, 'Techno-Economic Analysis of Lithium Extraciton from Geothermal Brines', **2021**, https://www.nrel.gov/docs/fy21osti/79178.pdf.

[23] J. M. Weinand, G. Vandenberg, S. Risch, J. Behrens, N. Pflugradt, J. Linßen, D. Stolten, *Adv. Appl. Energy* **2023**, *11*, 100148, https://doi.org/10.1016/j.adapen.2023.100148.

[24] T.-Y. Huang, J. R. Pérez-Cardona, F. Zhao, J. W. Sutherland, M. P. Paranthaman, *ACS Sustain. Chem. Eng*. **2021**, *9*, 6551, https://doi.org/10.1021/acssuschemeng.0c08733.

[25] M. A. Miranda, A. Ghosh, G. Mahmodi, S. Xie, M. Shaw, S. Kim, M. J. Krzmarzick, D. J. Lampert, C. P. Aichele, *Water* **2022**, *14*, 880, https://doi.org/10.3390/w14060880.

[26] E. Traver, R. A. Karaballi, Y. E. Monfared, H. Daurie, G. A. Gagnon, M. Dasog, *ACS Appl. Nano Mater*. **2020**, *3*, 2787, https://doi.org/10.1021/acsanm.0c00107.

[27] Z. Li, I.-C. Chen, L. Cao, X. Liu, K.-W. Huang, Z. Lai, *Science* **2024**, *385*, 1438, https://doi.org/10.1126/science.adg8487.

[28] N. Rivera-Gonzalez, A. Bajpayee, J. Nielsen, U. Zakira, W. Zaheer, J. Handy, T. Sill, B. Birgisson, M. Bhatia, S. Banerjee, *iScience* **2022**, *25*, 105063, https://doi.org/10.1016/j.isci.2022.105063.

[29] A. Battistel, M. S. Palagonia, D. Brogioli, F. La Mantia, R. Trócoli, *Adv. Mater*. **2020**, *32*, 1905440, https://doi.org/10.1002/adma.201905440.

[30] M. L. Vera, W. R. Torres, C. I. Galli, A. Chagnes, V. Flexer, *Nat. Rev. Earth Environ*. **2023**, *4*, 149, https://doi.org/10.1038/s43017-022-00387-5.

[31] J. Wang, G. M. Koenig Jr., *Chem. Eur. J.* **2024**, *30*, e202302776, https://doi.org/10.1002/chem.202302776.

[32] S. Fleischmann, J. B. Mitchell, R. Wang, C. Zhan, D.-e. Jiang, V. Presser, V. Augustyn, *Chem. Rev*. **2020**, *120*, 6738, https://doi.org/10.1021/acs.chemrev.0c00170.

[33] Y. Li, H. Chen, K. Lim, H. D. Deng, J. Lim, D. Fraggedakis, P. M. Attia, S. C. Lee, N. Jin, J. Moškon, Z. Guan, W. E. Gent, J. Hong, Y.-S. Yu, M. Gaberšček, M. S. Islam, M. Z. Bazant, W. C. Chueh, *Nat. Mater*. **2018**, *17*, 915, https://doi.org/10.1038/s41563-018-0168-4.

[34] Y. Luo, Y. Bai, A. Mistry, Y. Zhang, D. Zhao, S. Sarkar, J. V. Handy, S. Rezaei, A. C. Chuang, L. Carrillo, K. Wiaderek, M. Pharr, K. Xie, P. P. Mukherjee, B.-X. Xu, S. Banerjee, *Nat. Mater*. **2022**, *21*, 217, https://doi.org/10.1038/s41563-021-01151-8.

[35] D. Fraggedakis, N. Nadkarni, T. Gao, T. Zhou, Y. Zhang, Y. Han, R. M. Stephens, Y. Shao-Horn, M. Z. Bazant, *Energy Environ. Sci*. **2020**, *13*, 2142, https://doi.org/10.1039/D0EE00653J.
[36] M. Torkamanzadeh, C. Kök, P. R. Burger, P. Ren, Y. Zhang, J. Lee, C. Kim, V. Presser, *Cell Rep. Phys. Sci*. **2023**, *4*, 101661, https://doi.org/10.1016/j.xcrp.2023.101661.
[37] N. Holubowitch, A. Omosebi, X. Gao, J. Landon, K. Liu, *ChemElectroChem* **2017**, *4*, 2404, https://doi.org/10.1002/celc.201700082.
[38] A. Raveendran, M. Chandran, R. Dhanusuraman, *RSC Adv*. **2023**, *13*, 3843, https://doi.org/10.1039/D2RA07642J.
[39] X. Bu, Y. Zhang, H. Guo, S. Wang, X. Du, *Desalination* **2023**, *567*, 116982, https://doi.org/10.1016/j.desal.2023.116982.
[40] L. Herrmann, H. Ehrenberg, M. Graczyk-Zajac, E. Kaymakci, T. Kölbel, L. Kölbel, J. Tübke, *Energy Adv*. **2022**, *1*, 877, https://doi.org/10.1039/D2YA00099G.
[41] K. Ariyoshi, S. Masuda, *J. Electroanal. Chem*. **2023**, *943*, 117615, https://doi.org/10.1016/j.jelechem.2023.117615.
[42] C.-T. Hsieh, C.-T. Pai, Y.-F. Chen, P.-Y. Yu, R.-S. Juang, *Electrochimica Acta* **2014**, *115*, 96, https://doi.org/10.1016/j.electacta.2013.10.082.
[43] A. Siekierka, *Sep. Purif. Technol*. **2020**, *236*, https://doi.org/10.1016/j.seppur.2019.116234.
[44] E. J. Braham, R. D. Davidson, M. Al-Hashimi, R. Arróyave, S. Banerjee, *Dalton Trans.* **2020**, *49*, 11480, https://doi.org/10.1039/D0DT02028A.
[45] A. Mannodi-Kanakkithodi, G. Pilania, R. Ramprasad, T. Lookman, J. Gubernatis, *Comput. Mater. Sci*. **2016**, *125*, https://doi.org/10.1016/j.commatsci.2016.08.018.
[46] A. M. Gopakumar, P. V. Balachandran, D. Xue, J. E. Gubernatis, T. Lookman, *Sci. Rep.* **2018**, *8*, 3738, https://doi.org/10.1038/s41598-018-21936-3.
[47] J. Lee, S. Kim, C. Kim, J. Yoon, *Energ. Environ. Sci*. **2014**, *7*, 3683, https://doi.org/10.1039/c4ee02378a.
[48] N. I. Cool, R. James, P. Schofield, J. V. Handy, M. Bhatia, S. Banerjee, *ACS Appl. Mater. Interfaces* **2023**, *15*, 1554, https://doi.org/10.1021/acsami.2c17800.
[49] N. Xie, Y. Li, Y. Yuan, J. Gong, X. Hu, *ACS Appl. Energy Mater*. **2021**, *4*, 13036, https://doi.org/10.1021/acsaem.1c02654.
[50] B. Tansel, *Sep. Purif. Technol*. **2012**, *86*, 119, https://doi.org/10.1016/j.seppur.2011.10.033.
[51] J. V. Handy, Y. T. Luo, J. L. Andrews, N. Bhuvanesh, S. Banerjee, *Angew. Chem. Int. Ed*. **2020**, *59*, 16385, https://doi.org/10.1002/anie.202005513.
[52] X. Zhang, J. Chen, J. Ye, T. Zhang, Z. Hou, *Adv. Energy Mater*. **2023**, *13*, 2204413, https://doi.org/10.1002/aenm.202204413.
[53] F. Wang, L. Blanc, Q. Li, A. Faraone, X. Ji, H. Chen-Mayer, R. Paul, J. Dura, E. Hu, K. Xu, L. Nazar, C. Wang, *Adv. Energy Mater.* **2021**, *11*, 2102016, https://doi.org/10.1002/aenm.202102016.
[54] Y. Liu, J. Xu, J. Li, Z. Yang, C. Huang, H. Yu, L. Zhang, J. Shu, *Coord. Chem. Rev*. **2022**, *460*, 214477, https://doi.org/10.1016/j.ccr.2022.214477.
[55] A. B. Resing, C. Fukuda, J. G. Werner, *Adv. Mater*. **2023**, *35*, 2209694, https://doi.org/10.1002/adma.202209694.
[56] M. Ebner, D.-W. Chung, R. Garca, V. Wood, 'Tortuosity Anisotropy in Lithium-Ion Battery Electrodes Studied by Synchrotron X-ray Tomography', *ECS Meeting Abstracts*, **2013**. https://doi.org/10.1149/MA2013-01/7/409.
[57] C. D. Quilty, D. Wu, W. Li, D. C. Bock, L. Wang, L. M. Housel, A. Abraham, K. J. Takeuchi, A. C. Marschilok, E. S. Takeuchi, *Chem. Rev*. **2023**, *123*, 1327, https://doi.org/10.1021/acs.chemrev.2c00214.
[58] L. Guo, J. T. Zhang, M. Ding, C. D. Gu, S. Vafakhah, W. Zhang, D. S. Li, P. V. Y. Alvarado, H. Y. Yang, *Sep. Purif. Technol.* **2021**, *266*, https://doi.org/10.1016/j.seppur.2021.118593.
[59] Y. Liu, X. Gao, L. Zhang, X. L. Shen, X. Du, X. Y. Dou, X. Yuan, *Desalination* **2020**, *494*, https://doi.org/10.1016/j.desal.2020.114665.
[60] S. Wang, G. Wang, C. He, N. Gao, B. Lu, L. Zhao, J. Weng, S. Zeng, C. Li, *J. Mater. Chem. A* **2021**, *9*, 6898, https://doi.org/10.1039/D0TA11042F.
[61] L. Zhang, D. Zhou, G. He, Q. Yao, F. Wang, J. Zhou, *Mater. Lett*. **2015**, *145*, 351, https://doi.org/10.1016/j.matlet.2015.01.142.
[62] W. Y. Zhao, L. Guo, M. Ding, Y. X. Huang, H. Y. Yang, *Acs Appl. Mater. Inter.* **2018**, *10*, 40540, https://doi.org/10.1021/acsami.8b14014.
[63] J. Zhou, S. Xiang, X. Wang, D.-M. Shin, H. Zhou, *Chem. Eng. J.* **2024**, *482*, 148985, https://doi.org/10.1016/j.cej.2024.148985.
[64] D. Kaishentayev, B. Hascakir, 'SPE Annual Technical Conference and Exhibition 2021', https://doi.org/10.2118/206371-ms.
[65] B. R. Scanlon, R. C. Reedy, F. Male, M. Walsh, *Environ. Sci. Technol*. **2017**, *51*, 10903, https://doi.org/10.1021/acs.est.7b02185.
[66] L. D. Douglas, N. Rivera-Gonzalez, N. Cool, A. Bajpayee, M. Udayakantha, G.-W. Liu, Anita, S. Banerjee, *ACS Omega* **2022**, *7*, 1547, https://doi.org/10.1021/acsomega.1c06399.
[67] A. Bajpayee, N. Rivera-Gonzalez, E. J. Braham, T. E. G. Alivio, Anita, S. Alvi, C. Li, N. Cool, M. Al-Hashimi, L. Fang, S. Banerjee, *Adv. Eng. Mater*. **2022**, *24*, 2101524, https://doi.org/10.1002/adem.202101524.
[68] C. Li, B. Lee, C. Wang, A. Bajpayee, L. D. Douglas, B. K. Phillips, G. Yu, N. Rivera-Gonzalez, B.-j. Peng, Z. Jiang, H.-J. Sue, S. Banerjee, L. Fang, *Mater. Horizons* **2022**, *9*, 452, https://doi.org/10.1039/D1MH01672E.
[69] J. V. Handy, W. Zaheer, R. Albers, G. Agbeworvi, T. D. Boyko, V. Bakhmoutov, N. Bhuvanesh, S. Banerjee, *Matter* **2023**, *6*, 1125, https://doi.org/10.1016/j.matt.2023.01.028.
[70] L. R. De Jesus, J. L. Andrews, A. Parija, S. Banerjee, *ACS Energy Letters* **2018**, *3*, 915, 10.1021/acsenergylett.8b00156.
[71] Y. Liang, Y. Yao, *Nat. Rev. Mater*. **2023**, *8*, 109, https://doi.org/10.1038/s41578-022-00511-3.
[72] A. Mistry, T. Heenan, K. Smith, P. Shearing, P. P. Mukherjee, *ACS Energy Letters* **2022**, *7*, 1871, https://doi.org/10.1021/acsenergylett.2c00870.
[73] J. Wu, Z. Ju, X. Zhang, C. Quilty, K. J. Takeuchi, D. C. Bock, A. C. Marschilok, E. S. Takeuchi, G. Yu, *ACS Nano* **2021**, *15*, 19109, https://doi.org/10.1021/acsnano.1c06491.
[74] J. O. G. Posada, A. J. R. Rennie, S. P. Villar, V. L. Martins, J. Marinaccio, A. Barnes, C. F. Glover, D. A. Worsley, P. J. Hall, *Ren. Sust. Energy Rev*. **2017**, *68*, 1174, https://doi.org/10.1016/j.rser.2016.02.024.
[75] Y. Luo, S. Rezaei, D. A. Santos, Y. Zhang, J. V. Handy, L. Carrillo, B. J. Schultz, L. Gobbato, M. Pupucevski, K. Wiaderek, H. Charalambous, A. Yakovenko, M. Pharr, B. X. Xu, S. Banerjee, *Proc. Nat. Acad. Sci. U S A* **2022**, *119*, 10.1073/pnas.2115072119.
[76] G. A. Horrocks, M. F. Likely, J. M. Velazquez, S. Banerjee, *J. Mater. Chem. A* **2013**, *1*, 15265, https://doi.org/10.1039/c3ta13690f.
[77] J. V. Handy, J. L. Andrews, B. Zhang, D. Kim, N. Bhuvanesh, Q. Tu, X. Qian and S. Banerjee, *Cell Rep. Phys. Sci*. **2022**, *3*, https://doi.org/10.1016/j.xcrp.2021.100712.
[78] P. Schofield, Y. Luo, D. Zhang, W. Zaheer, D. Santos, G. Agbeworvi, J. D. Ponis, J. V. Handy, J. L. Andrews, E. J. Braham, A. R. Balakrishna, S. Banerjee, *ACS Energy Lett*. **2022**, *7*, 3286, https://doi.org/10.1021/acsenergylett.2c01868.
[79] Y. Zhang, A. Hu, D. Xia, S. Hwang, S. Sainio, D. Nordlund, F. M. Michel, R. B. Moore, L. Li, F. Lin, Y. Zhang, A. Hu, D. Xia, S. Hwang, S. Sainio, D. Nordlund, F. M. Michel, R. B. Moore, L. Li, F. Lin, *Nat. Nanotechnol*. **2023**, *18*, https://doi.org/10.1038/s41565-023-01367-6.
[80] P. Falun, L. Ngamwongwan, S. Singsen, M. Chotsawat, P. Komen, A. Junkaew, S. Suthirakun, *J. Phys. Chem. C* **2024**, *128*, 10774, https://doi.org/10.1021/acs.jpcc.3c08078.
[81] B. W. Byles, B. Hayes-Oberst, E. Pomerantseva, *Acs Appl. Mater. Inter.* **2018**, *10*, 32313, https://doi.org/10.1021/acsami.8b09638.
[82] P. Ridley, R. Andris, E. Pomerantseva, N. P. Kobayashi, A. A. Talin, A. V. Davydov, *Low-Dimensional Mater. Dev.* **2019**, 110851J, https://doi.org/10.1117/12.2529626.
[83] A. Hu, Y. Zhang, F. Yang, S. Hwang, S. Sainio, D. Nordlund, E. Maxey, Q. Dai, J. Gu, L. Li, F. Lin, *ACS Energy Letters* **2022**, *7*, 10.1021/acsenergylett.2c01186.
[84] N. Zhang, F. Cheng, Y. Liu, Q. Zhao, K. Lei, C. Chen, X. Liu, J. Chen, *J. Am. Chem. Soc*. **2016**, *138*, 12894, https://doi.org/10.1021/jacs.6b05958.
[85] K. J. Seonghwan, L. Jaehan, K. Choonsoo, Y. Jeyong, *Electrochim. Acta* **2016**, *203*, 265, https://doi.org/10.1016/j.electacta.2016.04.056.
[86] L. Agartan, B. Hayes-Oberst, B. W. Byles, B. Akuzum, E. Pomerantseva, E. Caglan Kumbur, *Desalination* **2019**, *452*, 1, https://doi.org/10. 10.1016/j.desal.2018.10.025.
[87] K. M. Shah, I. H. Billinge, X. Chen, H. Fan, Y. Huang, R. K. Winton, N. Y. Yip, *Desalination* **2022**, *538*, 115827, https://doi.org/10.1016/j.desal.2022.115827.
[88] A. N. Shocron, R. S. Roth, E. N. Guyes, R. Epsztein, M. E. Suss, *Environ. Sci. Technol. Lett*. **2022**, *9*, 889, https://doi.org/10.1021/acs.estlett.2c00551.

License and Terms

The definitive version of this article is the electronic one that can be found at https://doi.org/10.2533/chimia.2024.845